

# MODELING OF SURFACE ACOUSTIC WAVE CHEMICAL VAPOR SENSORS

Zdravko Živković<sup>1</sup>, Marija Hribšek<sup>1</sup> and Dejan Tošić<sup>2</sup>

<sup>1</sup>Institute Goša, Belgrade, Serbia

<sup>2</sup>School of Electrical Engineering, University of Belgrade, Belgrade, Serbia

**Key words:** SAW, surface acoustic wave, vapor sensor, polymer

**Abstract:** New approach to modeling and analysis of transversal surface acoustic wave (SAW) chemical vapor sensors is presented. The sensor is modeled as a two-port device with parts represented by equivalent circuits. Change of output voltage, or frequency, as a function of vapor concentration is calculated. The model is general and includes propagation losses which are usually neglected in analysis methods. Closed form expressions for vapor concentration estimations are obtained. Simulation results are compared to experimental data. The approach enables better insight in the sensor operation and therefore the optimal design of vapor sensors.

## Modeliranje SAW senzorja kemičnih hlapov

**Ključne besede:** SAW, površinski akustični valovi, senzor hlapov, polimer

**Izvleček:** V prispevku predstavimo nov pristop k modeliranju in analizi transverzalnega SAW senzorja kemičnih hlapov. Senzor z dvema priključkoma modeliramo z nadomestnimi vezji. Izračunavamo spremembo izhodne napetosti ali frekvence v odvisnosti od koncentracije hlapov. Model je splošen in upošteva izgube, ki jih druge analize zanemarijo. Simulacije primerjamo z merjenimi rezultati. Naš pristop omogoča boljše razumevanje delovanja senzorja zatoj tudi možnost optimalnega načrtovanja kemičnih senzorjev hlapov.

### 1. Introduction

In the last two decades surface acoustic wave (SAW) chemical vapor sensors have found numerous applications due to their compact structure, high sensitivity, small size, outstanding stability, low cost, fast real-time response, passivity, and above all their ability to be incorporated in complex data processing systems. They can be used for *in situ* monitoring and sensing systems. /1,2,3/

The basic principle of SAW sensors is the reversible sorption of chemical vapors by a solvent coating which is sensitive to the vapor to be detected. It is interesting that a SAW-based sensor system is used as a volatile organic contamination monitoring system for the satellite and space vehicle assembly rooms in NASA. SAW sensors have been able to distinguish organophosphates, chlorinated hydrocarbons, ketones, alcohol, aromatic hydrocarbons, saturated hydrocarbons, and water /1/. SAW sensors are particularly useful for wireless monitoring in harsh environment /4/.

Surface acoustic waves were discovered in 1885 by Lord Rayleigh and are often named after him as Rayleigh waves /5/. A surface acoustic wave is a type of mechanical wave motion which travels along the surface of a solid material, referred to as substrate. The amplitude of the wave decays exponentially with distance from the surface into the substrate, so that the most of the wave energy is confined to within one wavelength of the surface /6,7/. The velocity of acoustic waves is typically 3000 m/s, which is much lower than the velocity of the electromagnetic waves.

A basic SAW device was originally developed in 1965 /8/. It consists of two interdigital transducers (IDTs) on a piezo-

electric substrate such as quartz. Each IDT is a reversible element made of interleaved metal electrodes, which are used to launch and receive the waves: an electrical signal is converted to an acoustic wave and then back to an electrical signal. An IDT is a bidirectional transducer that radiates energy equally on both sides of the electrodes. Consequently, theoretical insertion loss introduced by an IDT is at least 6 dB.

Starting around 1970, different kinds of SAW devices were developed for applications in pulse compression radars, satellite communications and signal processing systems, mobile radio, and cellular telephones /9,10/. There are very broad ranges of commercial and military system applications that include components for radars, front-end and IF filters, CATV and VCR components, cellular radio and pagers, synthesizers and analyzers, navigation, computer clocks, tags, and many, many others /11,12/. SAW devices have found numerous applications outside their conventional fields, communications and signal processing. In the last two decades considerable work has been done in the development of SAW sensors of different types. High quality SAW filters are used as temperature, pressure and stress sensors /4,13/ as well as chemical and biosensors /14,15/. Generally, two types of chemical SAW sensors are used: transversal (or delay) and resonant.

Analysis of SAW devices can be approached to in three ways: (1) exact analysis by solving the wave equation, (2) approximate analysis by means of equivalent electro-mechanical circuits, and (3) approximate analysis via the delta function model /9, pp.55-122/. It is well known that the exact analysis of SAW devices using surface wave theory is very complex (even in the case of a free surface)

/6,7,10,14/. It starts from the second Newton's law and a set of partial differential equations. The equations are solved for the appropriate boundary conditions and relations between mechanical and electrical quantities of a piezoelectric substrate. In the most general case, e.g. in the presence of electrodes on the surface, the Maxwell's equations for the electromagnetic field should be taken into account, as well. Consequently, the exact analysis can be effectively applied only for IDTs with a small number of electrodes.

The simplest approximate method of analysis is based on the delta function model. It gives the results relatively fast, but its use is limited to small loads and substrates with lower coupling constants.

Better approximate methods use equivalent circuit models for IDTs, where the analysis tools known in electrical engineering can be applied. In these methods the accuracy depends on the complexity of the model. The closed-form solutions are derived for simple IDTs on quartz and lithiumniobate /9, pp.55-122,15/. Recent development of MEMS-based SAW chemical sensors, on new piezoelectric materials, also utilize equivalent circuits but only for modeling frequency characteristics of uniform IDTs /16,17/. In addition, closed-form solutions for more complex IDT structures have been developed by means of advanced electrical engineering analysis methods /18,19,20,21/.

One of the main objectives in a chemical sensor analysis is derivation of formulas which connect the change of electrical signals (e.g., voltages and frequency shifts) and chemical quantities (e.g., vapor concentration). The existing analysis approaches are usually: (a) the exact analysis via the wave equation /2,3,7/ and (b) the analysis based on published formulas derived from the wave equation /22,23/. The most complete treatment of the exact analysis has been reported in /7/. Generally, chemical SAW sensors have been analyzed mainly from the chemical point of view with less attention given to the relations between the electrical and chemical quantities and matching conditions at the electrical ports.

Typically, the analysis that is based on published formulas (which connect electrical signals and chemical compounds) neglects many properties of a real SAW delay line, such as propagation losses, technological constraints, and production tolerances. This is the reason why some researchers perform more experiments than needed, or have difficulties in explaining discrepancies between the expected and measured values /24/.

In this paper, a new modeling algorithm for the analysis of transversal chemical SAW sensors, based on the electrical equivalent circuit method, is presented. The algorithm develops in a straight forward manner explicit general relations between electrical signals, voltages or frequencies, and vapor detection estimations taking into account properties of real SAW devices, which are usually neglected. The whole sensor is modeled as a two-port network consisting of three

parts: (1) the input interdigital transducer, (2) the delay line that is the sensing part, and (3) the output interdigital transducer. The transducers are modeled as three-port networks and the delay line as a two-port network.

This paper focuses on the essential problem of modeling the delay line with acoustically thin films and the influence of the gas concentration on its behavior and, consequently, on the sensor's output voltage or frequency. The proposed algorithm is used for the vapor concentration estimation and the results are compared with the experimental data. It has been shown that the concentration prediction is better if the properties of practical SAW devices are properly taken into account, especially at higher center frequencies.

## 2. Principles of SAW Sensor Operation

A transversal SAW chemical sensor can be schematically presented as in Figure 1. It consists of two interdigital transducers on a piezoelectric substrate, such as quartz. Piezoelectric materials are anisotropic, which will yield different material properties versus the cut of the material and the direction of propagation. Commonly used substrates are ST-cut quartz and lithiumniobate. ST-cut quartz crystal is cut at a specified angle ( $0^\circ$ ,  $132.75^\circ$ ,  $0^\circ$ ) to the crystallographic axes so that it has a small or vanishing dependence of wave velocity upon temperature at room temperature /7/. The SAW propagation is in the x-direction with velocity  $v = 3158$  m/s. Usually, Y-cut lithiumniobate crystal is used. The propagation is in the z-direction with velocity  $v = 3488$  m/s, but the temperature dependence is not negligible.

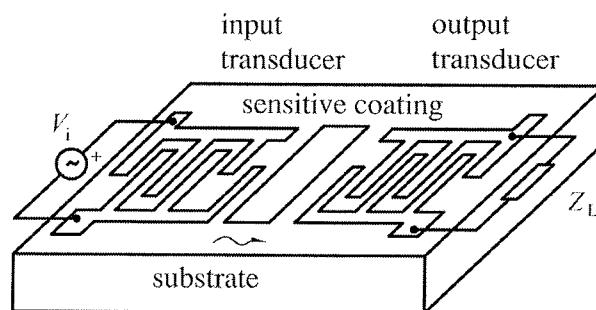


Fig. 1. The basic configuration of a chemical SAW sensor. (Acoustic absorbers and matching networks are not shown.)

A chemically sensitive thin layer is placed between the interdigital transducers on the top surface of the piezoelectric substrate. The surface wave is induced by an electrical signal applied to the input IDT.

The output signal (voltage) is taken from the output IDT. The velocity and attenuation of the wave are sensitive to mass and viscosity of the thin layer. The purpose of the thin layer – a polymer film – is to absorb chemicals of inter-

est. When the chemical is absorbed, the mass of the polymer increases causing a change in velocity and phase of the acoustic signal, which causes a change in amplitude and frequency of the output voltage at the load impedance  $Z_L$ . Acoustic absorbers (not shown in Figure 1) should be appropriately placed on the substrate edges to damp unwanted SAW energy and eliminate spurious reflections that could cause signal distortions.

The IDTs are identical with uniformly spaced electrodes of equal lengths and equal ratio of electrodes width and spacing. The number of electrodes defines the frequency bandwidth of a SAW device. The electrode's length and number, and matching networks at the electrical ports, should be chosen to match the IDT input resistance, at the center frequency  $f_0$ , to the load resistance  $R_L$  and the generator resistance  $R_g$ . In that case, the overall minimal loss due to IDTs is 12 dB. The wavelength corresponding to the center frequency equals the distance between the electrodes of the same polarity. The center frequency and the bandwidth are determined by the IDT's geometry and the substrate type.

The middle part of a SAW sensor is a delay line, generally treated as lossless. However, its losses can be neglected only for lower frequencies and small delays (small distances between the transducers). The transfer function of the delay line is normally assumed unity, although this may not be true for high frequencies ( $f > 0.5$  GHz) or if there are films in the propagation path [12, p.1.6-10]. In communications, in electrical filtering applications, the distance between the IDTs is small. Quite opposite, in chemical sensors this part is essential and must have a certain length, usually 100–200 wavelengths [7], which should be taken into account.

### 3. New Model of SAW Chemical Sensors

The configuration presented in Figure 1 can be modeled by a general equivalent electro-mechanical circuit given in Figure 2. The IDTs are three-port networks and the sensing part is a two-port network designated by DL in Figure 2. The characteristic SAW acoustic impedance of the unloaded substrate is designated by  $Z_0$  and the acoustic impedance due to the mass loading of the thin film is  $Z_m$ :

$$Z_0 = A\rho_s v \quad (1)$$

$$Z_m = A_m\rho_m v \quad (2)$$

where  $A$  is the substrate cross-section area through which the waves propagate,  $\rho_s$  is the mass density of the piezoelectric substrate,  $v$  is the SAW velocity in the piezoelectric substrate,  $A_m$  is the cross-section area of the thin film, and  $\rho_m$  is the mass density of the film.  $Z_g = R_g$  and  $Z_L = R_L$  are purely resistive electrical impedances of the generator and the electrical load, respectively.

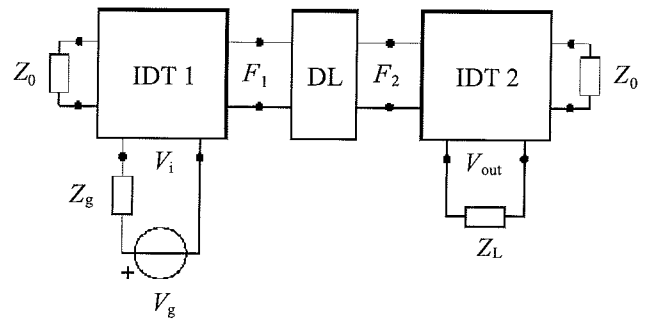


Fig. 2. The equivalent circuit of a SAW sensor.

Since the analysis of IDTs using equivalent electrical circuit models is well-known, the focus of this paper is to model the sensing part properties. The key observations relevant to the chemical sensor analysis are the following: (a) the sensor operates near the center frequency and (b) the IDTs are uniform with equal length electrodes. In that case, the IDT driving-point admittance at the electrical port,  $Y_{IDT} = G_a(f) + jB_a(f) + j2\pi f C_0$ ,  $j = \sqrt{-1}$ , where  $C_0$  is the static capacitance, can be calculated using well-known formulas [12, p.1.6-6/].

$$G_a(f_0) = 8k^2 f_0 C_s W_a N_p^2, \quad B_a(f_0) = 0 \quad (3)$$

where  $k$  is the piezoelectric coupling coefficient,  $f_0$  is the center frequency,  $C_s$  is the capacitance per unit electrode length,  $W_a$  is the electrode length (that is, the width of the wave front),  $N_p$  is the number of electrode pairs. Equation (3) is used for designing proper matching of IDTs at the electrical ports. It should be noted that the characteristics of IDTs outside the narrow band around the center frequency are of no interest.

The output voltage across the load  $V_{out}$  is proportional to the mass loading of the sensing part. First, the output voltage in the presence of sensing material (polymer without vapor) is calculated and it serves as a reference voltage  $V_b$ , also referred to as the baseline voltage. The difference of the output voltage in the presence of vapor and the reference voltage is proportional to the vapor concentration. In some applications the output voltage is directly measured, but usually the sensor is a part of a more sophisticated system. In that case two equal SAW sensors are used: one is vapor-free and serves as a reference, the other one is exposed to vapor and actually performs the sensing function. The two SAW sensors are embedded into electrical oscillator circuits and the frequency shift between the oscillators is proportional to the gas concentration. Using an electronic circuit called the mixer the voltage proportional to the vapor concentration is obtained from the frequency shift. In any case the voltage across the load has to be found, which implies that the electrical transfer function of the sensor has to be determined.

According to Figure 2 the electrical transfer function can be expressed as follows:

$$T(f) = \frac{V_{out}}{V_g} = \frac{V_{out}}{F_2} \frac{F_2}{F_1} \frac{F_1}{V_g} \quad (4)$$

where  $F_1$  and  $F_2$  are mechanical forces.

Since the transducers are identical,  $V_{out}/F_2$  is the conjugate complex value of  $F_1/V_g$ , and these terms are only functions of frequency. Therefore,

$$|T(f)| = |T_{13}(f)|^2 \left| \frac{F_2}{F_1} \right| \quad (5)$$

where  $T_{13}(f) = V_{out}/F_2$  represents the transfer function of the transducer. Fortunately, in this case, since the sensors work close to resonance in matched conditions at the input and output, the elaborate work of computing  $T_{13}(f)$  can be avoided. Instead of Eq. (5) a much simpler expression can be used:

$$|T(f_0)| = |T_{13}(f_0)|^2 \left| \frac{F_2}{F_1} \right| \quad (6)$$

At resonance, for a delay line without the polymer film, and negligible losses,  $F_2/F_1 = 1$  and  $|T_{13}(f_0)|^2 = 1/4 \approx -12\text{dB}$ . Therefore, the relative variation of the output voltage  $V_{out}$  due to the mass loading is equal to the relative variation of  $F_2$ . The delay line of Figure 2 can be schematically represented as shown in Figure 3.

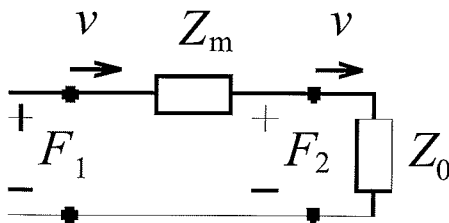


Fig. 3. The equivalent circuit of a mass loaded delay line.

By analogy between electrical and mechanical quantities, the relative variation of  $F_2$  and the relative variation of velocity, for  $Z_m$  much smaller than  $Z_0$ , are determined by

$$\frac{\Delta F_2}{F_{20}} = \frac{\Delta v}{v} = \frac{F_2 - F_{20}}{F_{20}} = \frac{-Z_m}{Z_0 + Z_m} \approx \frac{-Z_m}{Z_0} \Big|_{Z_m \ll Z_0} \quad (7)$$

where  $F_{20}$  denotes  $F_2$  without mass loading, and  $v$  is the corresponding wave velocity. Using Eqs. (6) and (7) the variation of the output voltage due to the mass loading, can be calculated as follows:

$$\frac{\Delta V_{out}}{V_0} = -\frac{Z_m}{Z_0} \quad (8)$$

Where  $V_0$  is the output voltage without the mass loading.

Using Eqs. (1),(2),(7),(8) and the well-known relationship between wavelength, velocity and frequency, the frequency shift due to the mass loading can be calculated as:

$$\frac{\Delta f}{f_0} = \frac{\Delta v}{v} = \frac{-Z_m}{Z_0} = \frac{\Delta V_{out}}{V_0} = -\frac{\rho_m h_m}{\rho_s \lambda_0} K_w \quad (9)$$

where  $\rho_m$  and  $h_m$  are the density and thickness of the thin layer,  $\rho_s$  is the density of the piezoelectric substrate, and  $K_w$  is a coefficient that depends on the technological process and implementation of the sensor.  $K_w$  is defined as the ratio of the polymer film width  $W_m$  and the width of the SAW front  $W_a$ :  $K_w = W_m/W_a$ . The components of the wave decay exponentially inside the substrate and the penetration is of the order of one wavelength. Therefore, in Eq.(9), instead of the substrate thickness, one wavelength  $\lambda_0$  is used. From the last equation  $\Delta f$  can be determined as:

$$\Delta f = -\frac{\rho_m h_m}{\rho_s v} f_0^2 K_w \quad (10)$$

The last equation shows that the higher sensitivity will be obtained if the center frequency is higher, thickness and density of the film larger, and the substrate density and velocity smaller. This means that quartz ( $\rho_s = 2.62 \text{ g/cm}^3$ ) is a better choice for the substrate than lithiumniobate ( $\rho_s = 4.7 \text{ g/cm}^3$ ). Furthermore, if ST-cut quartz is used temperature dependence can be neglected [7]. Using the last equation the frequency shift, or the output voltage change, due to the polymer sensing film (without vapor) can be determined:

$$-\frac{\Delta V_{out}}{V_0} = -\frac{\Delta f}{f_0} = \frac{\rho_p h_p}{\rho_s v} f_0 K_w \quad (11)$$

where  $\rho_p$  and  $h_p$  are the density and thickness of the polymer, respectively. The reference voltage is

$$V_b = V_0 - |\Delta V_{out}| = V_0 \left( 1 - \frac{|\Delta V_{out}|}{V_0} \right) \quad (12)$$

Since  $\Delta V_{out}$  is very small,  $V_b$  is very close to  $V_0$ .

Mass sensitivity  $S_m$  is an important characteristic of SAW sensors and is defined as  $S_m = \Delta f / \Delta(\rho_p h_p) / 22$ . According to Eq.(11), assuming  $K_w = 1$ , it follows:

$$S_m = \frac{\Delta f}{\Delta(\rho_p h_p)} = \frac{1}{\rho_s v} f_0^2 \quad (13)$$

The mass sensitivity is determined only by the substrate ( $\rho_s$  and  $v$ ) and the geometry of IDTs ( $f_0$ ).

When vapor is absorbed, an additional voltage change occurs. Using the same reasoning and the fact that  $h_p$  is much smaller than  $\lambda_0$ , the voltage change due to vapor in sorbent phase, can be calculated as

$$-\frac{\Delta V_{vap}}{V_b} = \frac{\rho_{vap} h_p}{\rho_s v} f_0 K_w \quad (14)$$

where  $\rho_{vap}$  is the density of the vapor in sorbent phase. The sorbent phase of a volatile chemical compound is that part of the compound which is absorbed by polymer. Since the reference voltage shift without vapor  $\Delta V_{out}$  is known, Eq.(11), the last equation can be expressed as follows:

$$\frac{\Delta V_{vap}}{V_b} = \frac{\rho_{vap}}{\rho_p} \frac{\Delta V_{out}}{V_0} \quad (15)$$

From Eq.(15) concentration of the chemical compound in vapor phase can be predicted using the known relation between the concentrations in sorbent and vapor phases /22/:

$$K = C_s / C_v \quad (16)$$

where  $K$  is the partition coefficient,  $C_s$  is the concentration of the chemical compound in sorbent phase (in the sorbent coating /14,p.291/), and  $C_v$  is the concentration of the chemical compound in vapor phase (concentration in the ambient /14,p.291/). Vapor sensitivity depends on the choice of the sorbent coating material, polymer, and its strength of sorption, which is given by the partition coefficient  $K$ . The voltage shift  $\Delta V_{\text{vap}}$  as a function of concentration  $C_v$  can be obtained as

$$\frac{\Delta V_{\text{vap}}}{V_b} = KC_v \frac{1}{\rho_p} \frac{\Delta V_{\text{out}}}{V_0} \quad (17)$$

The concentration in Eq.(17) is in  $\text{g/cm}^3$ . It should be noted that different concentration units can be used in literature, but the units used here are as in /14,p.291/. Consequently, the value of  $K$  depends on the concentration units used. Equivalent relationship holds for  $\Delta f$  and the frequency shift due to vapor  $\Delta f_{\text{vap}}$ :

$$\Delta f_{\text{vap}} = KC_v \Delta f / \rho_p \quad (18)$$

Equations (14)–(17) are derived for a delay line with negligible propagation losses. These equations contain normalized voltages (dimensionless quantities) so that they remain valid even for lossy delay lines. However, the propagation losses affect voltage shifts and voltages (quantities in Volts) and should be taken into account. The propagation loss is a nonlinear function of frequency, substrate and delay. According to /6,10/ the propagation loss for quartz can be calculated using

$$a_{1\mu\text{s}} = (2.15 f_{\text{GHz}}^2 + 0.45 f_{\text{GHz}}) \quad (19)$$

where  $a_{1\mu\text{s}}$  is the attenuation coefficient in  $\text{dB}/\mu\text{s}$  and  $f_{\text{GHz}}$  is the frequency in GHz. The propagation loss  $a_{\text{dB}}$  (in dB) is the product of the attenuation coefficient  $a_{1\mu\text{s}}$  and the delay  $\tau$  (in  $\mu\text{s}$ ):  $a_{\text{dB}} = a_{1\mu\text{s}} \tau$ . Any voltage  $V$  or a voltage shift  $\Delta V$  obtained from a lossless model should be divided by the factor  $a = 10^{a_{\text{dB}}/20}$ . If the desired accuracy in the voltage shift prediction is better than 1‰ (that is, better than 0.001), the propagation loss should be neglected only in the case when its value is less than 0.01 dB.

#### 4. Simulation Results and Discussion

Prediction of mass sensitivity as a function of frequency is demonstrated first.

For the quartz substrate ( $\rho_s = 2.62 \text{ g/cm}^3$ ,  $v = 3158 \text{ m/s}$ ), according to Eq.(13), the frequency dependence of the mass sensitivity is calculated and presented in Figure 4.

As can be seen, the simulation results, based on the proposed model, are in a good agreement with the experi-

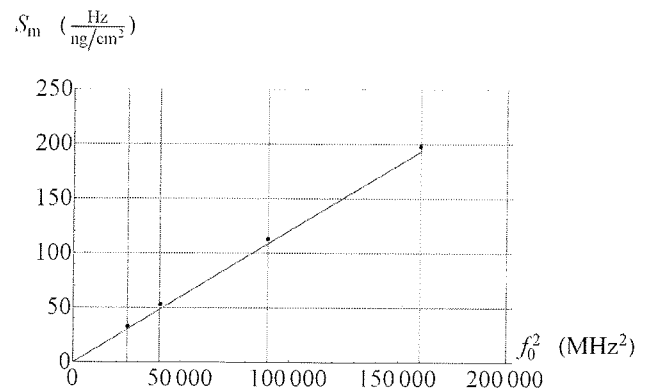


Fig. 4. Mass sensitivity versus  $f_0^2$ . Simulated results are represented by solid line and reported measured values /22, Figure 6/ are designated by dots.

mental results. The points in Figure 4 are obtained from Figure 6 reported in /22/ for the 158 MHz device of the transversal type and the (200, 300, 400) MHz devices of the resonator type.

Prediction of the frequency shift due to the polymer film on quartz is illustrated by the next example. Polymer is polyvinyl tetradecanal (PVTD) applied by Langmuir-Blodgett (LB) method /22/. Using Eq.(13), and the reported values for  $h_p = (79.5, 49.6, 22, 12.4) \text{ nm}$  and  $\rho_p = 1 \text{ g/cm}^3$ , the frequency shifts for four different center frequencies are calculated and presented in Table 1 along with the experimental results /22/.

Table 1. Frequency shifts due to polymer loading.

Frequency	158 MHz	200 MHz	300 MHz	400 MHz
Predicted $\Delta f$	240 kHz	240 kHz	239 kHz	240 kHz
Measured $\Delta f$	247 kHz	243 kHz*	250 kHz*	205 kHz*

The relative error in  $\Delta f$  is (probably) caused by the fact that the experimental values of  $h_p$  are higher than the reported calculated ones /22/, which were used in the prediction. The "\*" in Table 1 marks measured reported values for resonator type devices. However, the predictions are made for transversal devices, which explains the discrepancy between the experimental and predicted values at higher frequencies.

Finally, predictions of the frequency shift due to vapor are calculated. The polymer is PVTD and the vapor 1,2-dichloroethane (DCE). From Eq.(18) one can conclude that for the same polymer, vapor concentration, and  $\Delta f$  the same value of  $\Delta f_{\text{vap}}$  should be obtained regardless the center frequency.

For the vapor concentration of  $C_v = 650.8 \text{ g/m}^3$  and the center frequency of  $f_0 = 158 \text{ MHz}$ , the predicted frequency shift is  $\Delta f_{\text{vap}} = 16.6 \text{ kHz}$  and the measured shift is about 13 kHz /22/. The corresponding partition coefficient  $K = 10^{2.0279}$  is taken from the literature /1/.

The proposed algorithm is also applied to the calculation of vapor concentrations given in /1/. Vapor is trichloroethylene (TCE), and the polymer is PVTD. In this case, since the frequency is high, attenuation due to the propagation losses should be taken into account, but it does not effect the ratio  $\Delta V_{\text{vap}}/V_b$ . Using data from /1/ ( $f_0 = 500$  MHz,  $\log(K) = 2.65$ ,  $\rho_p = 0.96$  g/cm<sup>3</sup>,  $\Delta f = 1.5$  MHz,  $MW = 131.4$  g/mol,  $V_m = 24.46$  l/mol) and Eq.(17), the vapor concentration is calculated as a function of  $\Delta V_{\text{vap}}/V_b$ . The results are presented in Figure 5, where dots represent the measured data /1/. According to /1, Figure 3/ the correction factor is  $K_w = 0.76$ . The prediction is in a good agreement with the experimental results.

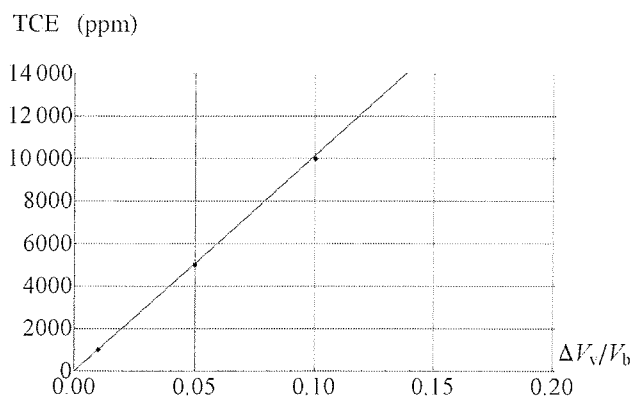


Fig. 5. TCE concentration versus the normalized voltage shift.

The proposed method is verified using experimental data from /24/. The experiments were carried out without any predictions, for devices on quartz at the center frequencies (39.6, 99, 132, 198, 264) MHz, different polymers, and three gases which simulate warfare chemical agents. Polymers were polyisobutylene (PIB), polyepichlorohydrin (PECH), and polydimethylsiloxane (PDMS) deposited by the spin coating technique. Space between the transducers was 1500 $\mu$ m with the aperture 1800 $\mu$ m. The characteristics were measured directly using E-5061A network analyzer.

Predictions are made at  $f_0 = 99$  MHz for PECH and dichloromethane (CH<sub>2</sub>Cl<sub>2</sub>, DCM) with  $\rho_p = 1.36$  g/cm<sup>3</sup>,  $h_p = 0.24$ mm,  $K = 10^{2.0743}$ ,  $MW = 85$  g/mol,  $V_m = 24.46$  l/mol. The delay  $\tau$  is calculated from the distance between transducers  $d_{\text{IDT}} = 1500\mu\text{m}$  and the wave velocity  $v = 3158$  m/s:  $\tau = d_{\text{IDT}}/v = 0.475\mu\text{s} \approx 0.5\mu\text{s}$ . The correction factor  $1/a$  due to attenuation loss is calculated according to Eq.(19),  $f_{\text{GHz}} = 0.099$ ,  $a_{1\mu\text{s}} = (2.15f_{\text{GHz}}^2 + 0.45f_{\text{GHz}})$ ,  $\tau = 0.5$ ,  $a_{\text{dB}} = a_{1\mu\text{s}}\tau$ ,  $a = 10^{a_{\text{dB}}/20}$ ,  $1/a = 0.996$ , as expected since the frequency is lower than 500 MHz and the delay is only about 0.5 $\mu$ s. For 5 ppm concentration of DCM, the predicted frequency shift is 584 Hz and the measured value is 574 Hz /24/.

Difficulties were encountered in measuring the concentration of the same gas on PIB /24/. That can be explained

by the proposed model: the constant  $K$  for PIB is about three times smaller than for PECH and therefore the detected voltage, which represents the gas concentration, will be also three times smaller, which gives insufficient voltage for the analyzer to be detected.

## 5. Conclusions

A new model for acoustically thin SAW transversal chemical vapor sensors has been developed. The model is based on electrical equivalent circuits of SAW devices, which connect electrical signals and chemical compounds, and takes into account important properties of real SAW devices, such as propagation losses, technological constraints, and production tolerances. The unique feature of the model is a set of closed form analytic expressions for vapor concentration estimations. The expressions explicitly relate the vapor concentration, substrate parameters, and center frequency. They enable insight into the influence of the sensor design parameters on the sensor performance.

The presented method predicts very efficiently and correctly the frequency and voltage shifts due to the vapor concentrations in chemical sensors. The simulation results, based on the proposed model, are in a good agreement with the experimental results. The results presented can be used in future for the design of optimal sensors for a given vapor.

## Acknowledgements

The authors would like to thank the Ministry of Science and Technological Development of Serbia for financial support under the project number TR 11026.

## References

- /1/ Ho, C.K.; Lindgren, E.R.; Rawlinson, K.S.; McGrath, L.K.; Wright, J.L. Development of a Surface Acoustic Wave Sensor for In-Situ Monitoring of Volatile Organic Compounds. *Sensors* 2003, 3, 236-247.
- /2/ Wohltjen, H.; Dessy, R. Surface acoustic wave probe for chemical analysis. *Analytical Chemistry* 1979, 51, 1458-1464.
- /3/ Wohltjen, H. Mechanism of operation and design considerations for surface acoustic wave device vapour sensors. *Sensors and Actuators* 1984, 5, 307-325.
- /4/ Pohl A. A Review of Wireless SAW Sensors. *IEEE Transactions on Ultrasonics, Ferroelectrics, and Frequency Control* 2000, 47, 317-332.
- /5/ Rayleigh L. On waves propagated along the plane surface of an elastic solid. *Proc. London Math. Soc.* 1885, 17, 4-11.
- /6/ Farnell, G.W. Elastic Surface Waves. In *Surface Wave Filters*; Matthews, H., Ed.; John Wiley: New York, USA, 1977; pp. 1-55.
- /7/ Martin, S.J.; Frye, G.C.; Senturia, S.D. Dynamics and Response of Polymer-Coated Surface Acoustic Wave Devices: Effect of Viscoelastic Properties and Film Resonance. *Analytical Chemistry* 1994, 66, 2201-2219.
- /8/ White, R.M.; Voltmer, F.W. Direct Piezoelectric Coupling to Surface Electric Waves. *Appl. Phys. Lett.* 1965, 7, 314-316.

- /9 / Matthews, H. Surface Wave Filters; John Wiley: New York, USA. 1977; pp. 443-476.
- /10 / Morgan, D.P. Surface Wave Devices for Signal Processing; Elsevier: London, UK. 1985; pp. 15-57.
- /11 / Campbell, C. Surface Acoustic Wave Devices and their Signal Processing Applications; Academic Press: San Diego, USA. 1989, pp. 238-315.
- /12 / Golio, M. The RF and Microwave Handbook, Second Edition; CRC Press LLC: Boca Raton, USA. 2008; pp. 1.6.1-1.6.15.
- /13 / Seifert, F.; Bulst, W.E.; Ruppel, C. Mechanical sensors based on surface acoustic waves. Sensors and Actuators 1994, A44, 231-239.
- /14 / Ballantine, D.S.; White, R.M.; Martin, S.J.; Ricco, A.J.; Zellers, E.T.; Frye, G.C.; Wohltjen, H. Acoustic Wave Sensors: Theory, Design, Physico-Chemical Applications; Academic Press: San Diego, USA. 1997, pp. 1-7.
- /15 / Smith, W.R., et al. Analysis of interdigital surface wave transducer by use of equivalent circuit model. IEEE Transaction on Microwave Theory and Techniques 1969, 17, 856-864.
- /16 / Rufer, L.; Torres, A.; Mir, S.; Alam, M. O.; Lalinsky, T.; Chan, Y. C. SAW chemical sensors based on AlGaIn/GaN piezoelectric material system: acoustic design and packaging considerations, in Proceedings of the 7<sup>th</sup> International Conference on Electronics Materials and Packaging, EMAP 2005, 2005, Tokyo, Japan, pp. 204-208.
- /17 / Rufer, L.; Lalinsky, T.; Grobelný, D.; Mir, S.; Vanko, G.; Ōszi, Zs.; Mozolová, Ž.; Gregus, J. GaAs and GaN based SAW chemical sensors: acoustic part design and technology, in Proceedings of the 6<sup>th</sup> International Conference on Advanced Semiconductor Devices and Microsystems, ASDAM 2006, 2006, Smolenice, Slovakia, pp. 165-168.
- /18 / Debnath, N.; Ajmera, J.C.; Hribšek, M.F.; Newcomb, R.W. Scattering and Admittance Matrices of SAW Transducers. Circuits, Systems and Signal Processing 1983, 2, 161-178.
- /19 / Hribšek, M.; Tošić, D. An Improved Algorithm for Analysis of Uniform SAW Devices, in Proceedings of the 26<sup>th</sup> Midwest Symposium on Circuits and Systems, 1983, Puebla, Mexico, pp. 243-246.
- /20 / Hribšek, M.; Tošić, D. An Improved algorithm for Analysis of SAW Pulse Compression Filters, in Proceedings of the 8<sup>th</sup> Microcoll Conference, 1986, Budapest, Hungary, pp. 373-374.
- /21 / Hribšek, M. Transfer Function of a SAW Device with Apodized Transducers, in Proceedings of the International Symposium on Circuits and Systems ISCAS'82, 1982, Rome, Italy, pp. 636-638.
- /22 / Grate, J.W.; Klusty, M. Surface Acoustic Wave Vapor Sensor Based on Resonator Devices, NRL Memorandum report 6829, May 23, 1991, pp. 1-38.
- /23 / Grate, J.W.; Zellers, E.T. The Fractional Free Volume of the Sorbed Vapor in Modeling the Viscoelastic Contribution to Polymer-Coated Surface Acoustic Wave Vapor Sensor Responses. Analytical Chemistry 2000, 72, 2861-2868.
- /24 / Joo, B.-S.; Lee, J.-H.; Lee, E.-W.; Song, K.-D.; Lee, D.-D. Polymer Film SAW Sensors for Chemical Agent Detection, in Proceedings of the 1<sup>st</sup> International Conference on Sensing Technology, Nov. 21-23, 2005, Palmerston North, New Zealand, pp. 307-310.

Zdravko Živković, Marija Hribšek \*  
Institute Goša, Milana Rakića 35, 11000 Belgrade,  
Serbia. E-Mail: zdravko.zivkovic@ymail.com

Dejan Tošić  
School of Electrical Engineering, University of  
Belgrade, Bulevar kralja Aleksandra 73, PO Box 35-54,  
11120 Belgrade, Serbia. E-Mail: tosic@etf.rs

\* Corresponding author: marija.hribsek@yahoo.com;  
tel.: +381-11-2413332; fax: +381-11-2410977

Prispelo (Arrived): 20.02.2009 Sprejeto (Accepted): 09.06.2009